Asian Journal of Chemistry; Vol. 30, No. 4 (2018), 845-852

ASIAN JOURNAL OF CHEMISTRY

https://doi.org/10.14233/ajchem.2018.21088

A Comparative Photocatalytic Activity of $LiNbO_3$ and TiO_2 by Investigating the Removal Efficiency of Toluene from Indoor Air

RANJIT K. NATH[1,2,*], RAJIA SULTANA[1], ROKSANA KHATUN[1], RASHADUL HOSSAIN[1] and M.F.M. ZAIN[2]

[1]Department of Chemistry, Faculty of Engineering & Technology, Chittagong University of Engineering and Technology (CUET), Chittagong-4349, Bangladesh
[2]Sustainable Construction Materials and Building Systems (SUCOMBS) Research Group, Faculty of Engineering and Built Environment, Universiti Kebangsaan Malaysia, 43600 UKM Bangi, Malaysia

*Corresponding author: E-mail: rkn_chem@yahoo.com

Received: 13 October 2017; *Accepted*: 4 January 2018; *Published online*: 28 February 2018; AJC-18798

The quality of the indoor environment has become a major health consideration, because air pollution can be several times higher than outdoors. Photocatalytic materials can remove air borne contaminants like, volatile organic compounds (VOCs) that may toxic and harmful for human health. In this study, lithium niobate ($LiNbO_3$) and titanium dioxide (TiO_2) were used as catalyst to compare their efficiencies in degradation and absorption of toluene. Toluene was used as a model of volatile organic compound that can be found in indoor environment. Experiments were conducted in a photocatalytic test reactor, utilizing concrete blocks coated with $LiNbO_3$ and TiO_2 under UV light. Different concentrations of toluene were loaded and passed through the photocatalytic reactor and the removal efficiency of volatile organic compound was determined by GC-FID and GC-MS multi-analyzer. The findings demonstrate the stronger adsorption capacity and higher photodegradation efficiency can be achieved by $LiNbO_3$ more than TiO_2.

Keywords: Photocatalysts, Photodegradation, Volatile organic compounds, Toluene, Indoor air purification, Air-cleaning.

INTRODUCTION

Indoor air quality is a major concern in recent years as people spend more of their time in indoors. The quality of indoor air can be deteriorated by a variety of pollutants such as microbial contaminants, volatile and semi volatile organics that can affect the comfort level of air and induce public health problem that threatens virtually all workers in offices and buildings. In most of the urban areas, source control is often ungovernable and unavoidable [1,2]. These pollutants are emitted from different sources such as vehicular exhaust from nearby traffic, biological contaminants, tobacco smoke, indoor activities such as cooking, household products, cooling and heating systems [3,4].

The quality of indoor air has a direct impact on human health in terms of lengthened exposure to pollutants by breathing. Subsequent to the oil crisis in 1970s, buildings were designed to be more energy efficient with better insulation [5,6]. This means that a lower air exchange rate is used and the pollutant concentration accumulated are often higher than the outdoor environment. The health effects of organic chemicals at low or moderate concentrations in the air can cause breathing problems, trigger asthma and reduce lung function. This phenomenon is known as 'Sick Building Syndrome' (SBS) [7-9] and these occurrences lessened when the occupants started vacating such buildings [10].

Advanced oxidation process (AOP) such as photocatalysis, is a promising technology for air cleaning. Photodegradation occurs at room temperature and pressure, in fact oxidation of pollutants to H_2O and CO_2, no additional carrier gas is needed [11-14]. Heterogeneous photocatalysis with TiO_2 as catalyst is a rapidly developing field in environmental engineering. In the past decade, the removal of trace levels of inorganic and organic contaminants in air through a photocatalytic process has received much attention because of this technology is potentially suitable for air purification in office buildings and residences [15,16]. Coating photocatalyst modified concrete materials on the external surface of buildings may be a good supplement to conventional technologies to treat the gaseous exhaust emission [17,18]. The European Union since few years has supported an international research consortium, 'Photocatalytic Innovative Coverings Applications for Depollution Assessment (PICADA)' that has investigated the use of building materials to reduce air pollution [19-21]. The application of TiO_2 as an air purifier in the presence of the sunlight or ultraviolet (UV) radiation was first introduced at Japan in 1996

[22,23]. The versatile function of TiO_2, which can both serve as photocatalytic materials and coating materials, has facilitated its application in exterior construction materials and interior materials, such as cement mortar, exterior tiles, paving blocks, glass and PVC fabric [24-26]. In presence of the UV radiation (wavelength < 375 nm) TiO_2 generates hydroxyl free radicals ($^{\bullet}OH$) which is a strong oxidizing agent, that can degrade or oxidize the pollutants, such as toxic and bioresistant substances into more environmental friendly products as harmless and non-toxic gases.

The current study was conducted to investigate the efficiency performance of photocatalytic materials on the technique of producing concrete block, using local waste materials [27,28]. It was conducted for solving the problem of the increasing rates of volatile organic compounds in indoor air.

EXPERIMENTAL

Pollutant concentration and analytical methods: Toluene was selected as the target volatile organic pollutant. The pollutant concentrations were carefully and specifically selected, because the pollutant concentration has an essential effect on various aspects of photocatalysis. Most of the photocatalytic studies were conducted using a concentration of more than hundreds parts-per-million (ppm) level [29,30]. In this study, the concentration of target pollutants are selected with reference to the typical indoor air pollutant level and most of the experiments conducted within the concentration range 210-520 ppm. Gas chromatography-flame ionization detector (GC-FID) and gas chromatography-mass spectrometer (GC-MS) were used for measurement of toluene adsorption and degradation followed by scanning electron microscope (SEM) of the catalyst for a clear illustration of changes that happened to photocatalytic particle structure on the surface of the samples. The experimental set up involves removal of toluene as a target pollutant removal from indoor air at ambient conditions of temperature 25-27 °C, relative humidity at 50-55 % and residence times spanned from 6 to 7 h.

Mix proportions: Concrete blocks with different mixing were made in the laboratory. Two methods proposed for application of TiO_2 and $LiNbO_3$ into concrete blocks; one of these methods is adding the photocatalyst (TiO_2 and $LiNbO_3$) on the surface layer of concrete mix during preparation the block and the other one is coating (1 mm) layer of photocatalyst on the surface of concrete block. Mixes with varying cement to sand to aggregate (C:S:A) ratios for photocatalytic concrete blocks were 1:2:4, 1:2:3 and 1:3:6 prepared. The mixes were prepared by utilizing tab water with water to cement (W/C) ratio 0.5. The mixes by adding photocatalyst to the concrete surface layer were prepared with two layers; surface and basic layer. The surface layer mix was prepared with cement, sand, water and a certain amount of TiO_2 or $LiNbO_3$ (illustrated by the character b in Table-1). Furthermore, basic layer was prepared with cement, coarse aggregate (CA), water and sand (illustrated by the character a in Table-1), using weight as a design method for all samples preparation. Fig. 1 shows the concrete block design by adding a catalyst to the first layer of concrete mixing.

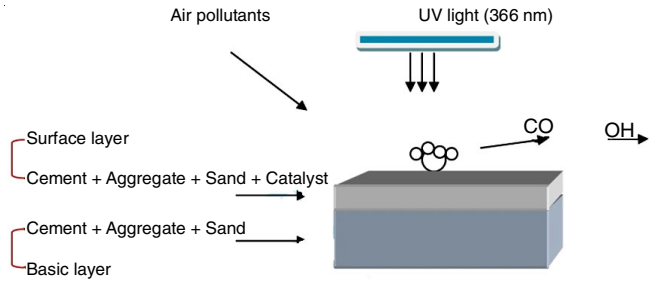

Fig. 1. Illustrated the photocatalytic concrete block materials and catalyst applied method

The other type of photocatalytic concrete blocks was coated with a 1 mm layer of target catalyst on the concrete surfaces. Mixes of coating photocatalytic concrete block surfaces were prepared as one block with cement, coarse aggregate, water and sand with using weight as a design method. Details of the concrete mixes prepared with different materials are provided in Table-1.

Photocatalytic test setup: All adsorbtion and degradation processes of toluene were carried out in a semi-batch reactor. It is the core part of the experimental setup; and allowed by concrete sample of the size 10 cm × 20 cm to be fixed. The reactor is made from stain steel material which is non-absorbing to the applied pollutant and can hold up UV-light of high irradiance. The reactor is tightly closed with a glass plate made from borosilicate glass to allow the UV-light radiation to pass

TABLE-1
DETAILS OF MIX PROPORTIONS FOR PHOTOCATALYTIC CONCRETE PREPARED WITH DIFFERENT MATERIALS AND LAYERS; (a) MIXES OF BASIC LAYER AND (b) MIX OF THE SURFACE LAYER

Types	Mix ratio	Relative properties (by weight)					
		Cement (Kg)	Sand (Kg)	CA (Kg)	TiO_2 (g)	$LiNbO_3$ (g)	Water W/C
a	1:2:4	6	10	20	4.72	3.56	0.5
b	1:2:4	6	10	20			
b	1:2:4	6	10	20			
b	1:2:4	6	10	20			
a	1:2:3	7	11.70	18.20	4.72	3.56	0.5
b	1:2:3	7	11.70	18.20			
b	1:2:3	7	11.70	18.20			
b	1:2:3	7	11.70	18.20			
a	1:3:6	4.26	10.53	21.87	4.72	3.56	0.5
b	1:3:6	4.26	10.53	21.87			
b	1:3:6	4.26	10.53	21.87			
b	1:3:6	4.26	10.53	21.87			

through with almost no restriction and rubber was used to consolidate the reactor. The surface of the sample is fixed parallel to the covering glass inside the reactor, leaving a slot of 0.3 cm for the gas to pass through it; the sample gas only passes the reactor through the slot between the sample surface and the glass cover in longitudinal direction. In this study two10W UV-lamps (model UVL-56, Agilent Technologies, USA) with wavelengths 366 nm were used to supply the irradiation to concrete surface for activating the photocatalyst. In addition, a small fan was used for air circulation and sensors were used for monitoring temperature and humidity.

Kinetic modeling of photocatalytic oxidation reaction: The data collection procedure used in the kinetic study of the adsorption and photodegradation reaction is the same as in the photoactivity measurements. The photoreactor was vacuumed before injecting a quantified gas sample. After preparing the samples and placed in the reactor, the target pollutants were injected until the concentration attained, then UV illumination was started. The total illumination time of each photodegradation process is 6 to 7 h. Each sample was analyzed after every 20 min irradiation time. The amount of toluene removal is calculated by using the following equation:

$$Q_{pol_x} = \frac{\int([pol]_o - [pol])dt}{A \times T} \quad (1)$$

where, Q_{pol_x}: The amount of pollution removed by the test sample ($mgL^{-1}\ m^{-2}\ h^{-1}$); $[Pol]_o$: injected concentration of pollutant (mg/L); [Pol]: pollutant concentration after adsorption (mg/L); dt: time of removal operation (min); A: surface area of concrete block samples (m^2); T: duration of the photocatalytic process, 7 h for all experiments.

This is Langmuire Hinshelwood (L-H) model which is widely used to describe the kinetics of gas solid phase reaction in heterogeneous photocatalysis. It can be applied to analyze the degradation rate of volatile organic compounds conversion in the photocatalytic concrete blocks.

RESULTS AND DISCUSSION

Photocatalytic removal of toluene from indoor air: Table-2 shows the photoactivity of TiO_2 and $LiNbO_3$ on the photocatalytic oxidation of toluene while Figs. 2 and 3 gave the graphical presentation. TiO_2 and $LiNbO_3$ had an increasing curve trend then gradually decreases with time until the value of the curve be constant.

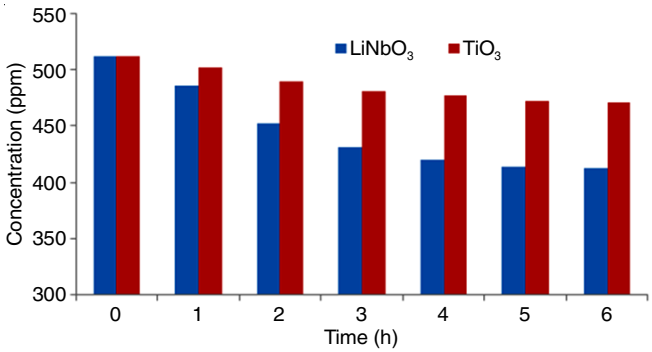

Fig. 2. High concentration runs of toluene adsorption for $LiNbO_3$ and TiO_2 coated on the surface of concrete blocks after 7 h

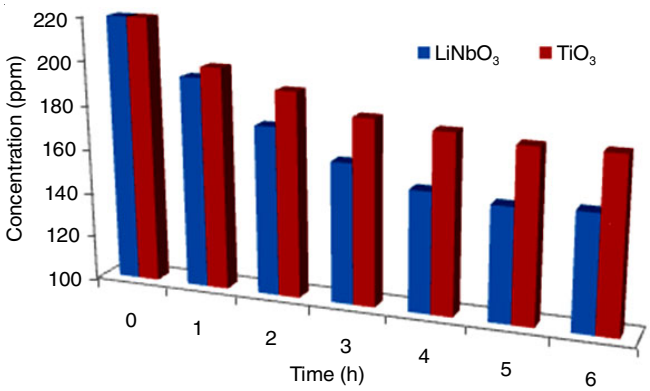

Fig. 3. Low concentration run of toluene adsorption for $LiNbO_3$ and TiO_2 coated on the surface of concrete blocks after 7 h

The TiO_2 shows the ability to adsorb low and high concentration of toluene. At high and low concentration of toluene it adsorbed about 8.6 % and 14.7 % of toluene within 4 h, respectively. It has been reported [31] that photodegradation of toluene using 2 g TiO_2 coated on plate reactor can degrade 10 % at low toluene concentration. Zhang and co-workers [32] found different result, about 20 % adsorption of toluene conducted in a gas-solid system using polycrystalline anatase TiO_2. Although, Pichat *et al.* [33] observed a 75 % toluene oxidation using TiO_2 anatase, where the initial toluene concentration used in the study was 60 pL.

A positive effect of $LiNbO_3$ shows on the photocatalytic activity in comparison to TiO_2. The photocatalytic oxidation of both low and high concentrations of toluene increased with $LiNbO_3$ compared to TiO_2. $LiNbO_3$ and TiO_2 have a clear impact on toluene removal in both high and low concentrations.

TABLE-2
TOLUENE REMOVAL RATE AFTER 7 h FROM THE TIME INTRODUCED INTO A CHAMBER AT 25-27 °C, RELATIVE HUMIDITY 50-55 % AT LOW (210 ppm) AND HIGH (520 ppm) $[Pol]_o$ CONCENTRATIONS

Sampling time (h)	GC peak area (m^2)	TiO_2 Pol_1 (ppm)		TiO_2 $Q(Pol_x)$ (ppm m^{-2} h^{-1})		$LiNbO_3$ Pol_1 (ppm)		$LiNbO_3$ $Q(Pol_x)$ (ppm m^{-2} h^{-1})	
		Low	High	Low	High	Low	High	Low	High
0	0.02	210	520	0	0	210	520	0	0
1	0.02	200	508	500	600	194	482	800	1900
2	0.02	195	498	3000	4400	181	468	5800	10400
3	0.02	186	482	10800	17100	170	448	18000	32400
4	0.02	179	475	24800	36000	158	429	41600	72800
5	0.02	179	468	38750	65000	158	429	65000	113750
6	0.02	179	468	55800	93600	158	429	93600	163800
7	0.02	179	468	75950	127400	158	429	127400	222950

Pol_1: Toluene concentration after adsorption; $Q(pol_x)$: Toluene removal rate; $[Pol]_o$ = Injected conc. of toluene.

With a low concentration of toluene (21.4 %) was adsorbed within 2 h using $LiNbO_3$, compared with TiO_2 which takes about 5 h to adsorb the same amount of toluene. At high concentration of toluene, $LiNbO_3$ showed high photoreactivity, about 21.1 % of toluene was adsorbed within 4 h, whereas, the same amount of toluene was adsorbed in 6 h by TiO_2. The results were also illustrated high concentrations of toluene adsorption after 7 h for both high and low concentrations, about 17.5-24.7 % and 10-14.7 % of toluene adsorbed by $LiNbO_3$ and TiO_2, respectively. From this result, it is shown that the rate of photocatalytic oxidation is dependent on the concentration of the pollutants. The lower of the toluene concentration is a better photocatalytic oxidation rate and the higher removal of toluene. This is an obvious observation where is the amount of toluene oxidized depending on the amount of radicals on the catalyst, which in turn depends on the number of holes generated on the catalyst [28]. Therefore, with a lower concentration of toluene the radicals generated by the holes is sufficiently high and enough to degrade the low quantity of toluene. But with higher concentration of toluene, the amounts of the radicals are insufficient to degrade all toluene.

The toluene oxide reaction dispersed on the TiO_2 surface can involve some charge transfer with $LiNbO_3$ during illumination due to the difference in the energy band position. As the valence band of TiO_2 is lower than that of $LiNbO_3$, this can promote the charge separation of the generated carriers. The charge transfer process can also be promoted, as more of the Nb^+ ions were distributed near the surface because of the larger $LiNbO_3$ particle size compare to TiO_2, hole trapping will be easier and this will improve the photocatalytic activity of $LiNbO_3$ by forming more ions radicals will be formed [34,35].

Additionally, the photodegradation of toluene by $LiNbO_3$ and TiO_2, a different pathway was suggested to be involved in the oxidation of toluene. The removal effect of TiO_2 and $LiNbO_3$ can be attributed to the fact that these catalysts create acceptor and donor surface sites (the source molecule from which the charge is transferred is called the electron donor and the receiving species is called the electron acceptor) [36]. Furthermore, as the sizes of these catalysts are smaller, most of these catalysts will work on adsorption pollutants effectively. This will increase the probability of electron-hole recombination and thus re-produce the photocatalytic activity of $LiNbO_3$ and TiO_2.

Photocatalytic degradation of toluene: As a measure of air purification potential, ZnO and TiO_2 activity toward toluene photodegradation was conducted at ambient conditions of temperature 25-27 °C and air relative humidity was 50-55 %. Figs. 4 and 5 shows the graphical presentation of degradation data for high and low concentration of toluene under UV-light (λ = 366 nm) after 7 h of exposure.

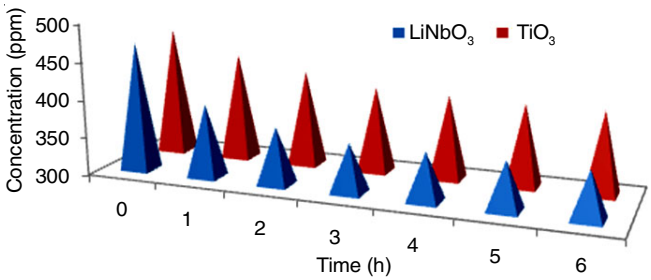

Fig. 4. Toluene degradation rate using $LiNbO_3$ and TiO_2 thin layer coating on the concrete block surface after 7h exposure for concentration = 520 ppm

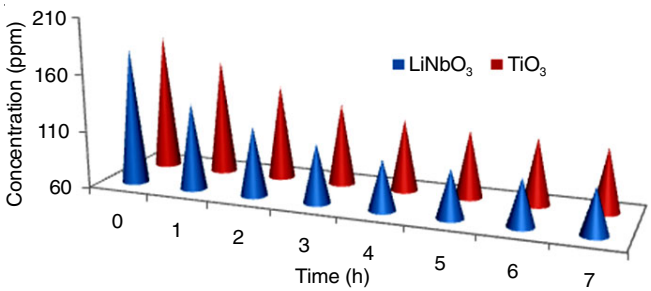

Fig. 5. Toluene degradation rate using $LiNbO_3$ and TiO_2 thin layer coating on the concrete block surface after 7 h exposure for concentration = 210 ppm

As shown in these figures, the photocatalyst TiO_2 and $LiNbO_3$ samples show relatively high degradation ability for toluene, while a decrease trend is observed after 4 h. The degradation ability increases rapidly in the first hour and reach stability within 5-7 h for both catalysts. This result confirms that the organic pollutant with different concentrations is easier to be degraded through photocatalysts [37]. Fig. 6 shows the GC-Mass analysis result of toluene using Agilent 7890A system at retention time 4.134 min.

From the results obtained, degradation efficiency of toluene with catalyst coated on the surface of concrete blocks is more useful compared to that of added catalyst to the concrete surface mixes at similar conditions. As an illustration of a typical experiment, Fig. 7 shows the result of products identified during the

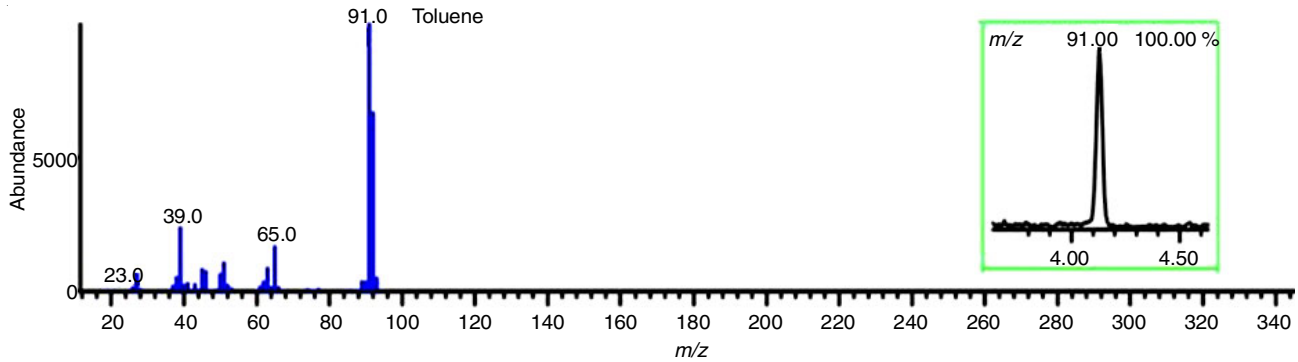

Fig. 6. Chromatogram and mass spectrum (GC-MS) of photodegradation product reveal the retention time of toluene and confident of more than 98 % matching quality using the NIST library

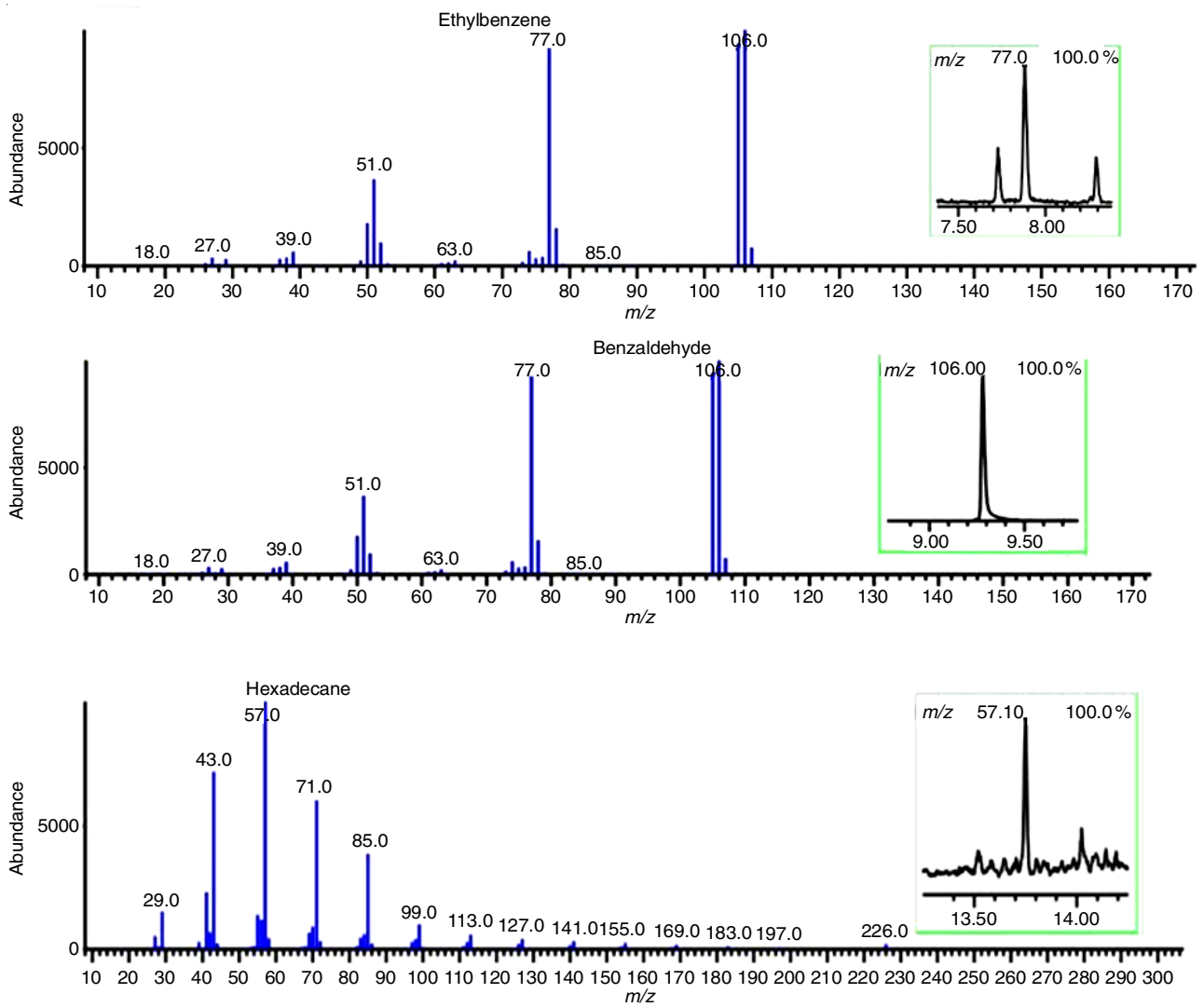

Fig. 7. Toluene degradation products identified by GC-MS chromatograms on the $LiNbO_3$ and TiO_2 under UV-light irradiation (366 nm) and confident of more than 98 % matching quality using the NIST library

degradation of toluene of the coated surface samples under UV-light irradiation. Table-3 summarized the degradation data of these products. Each compound identified with > 95 % confidence according to the mass spectral reference library of the National Institute of Standards and Technology (NIST). As it was expected, in the absence of near UV-irradiation, no significant toluene removal or degradation was observed. Under irradiation of UV-light, toluene behaved as unstable on the catalyst surface. Its concentration gradually decreased, and an amount of CO_2 was generated during the reaction. And that, the addition of photocatalyst could accelerate the degradation rate, more than 55 % of toluene vapour was degraded upon 7 h under UV-irradiation at high and low concentration, but only 16 % of which was degraded into CO_2. In addition, degradation rate of toluene was much faster at low toluene concentration. Similar results have been reported by Wang and Ray [38], in their study on chlorine radical and hydroxyl radical reactivates with toluene and benzene and found that toluene is 13 times more reactive than benzene with chlorine radicals, but much closer reactivates between toluene and benzene are observed with only in presence of hydroxyl radicals.

As shown in Fig. 7, toluene degradation intermediate organic products that detected by GC-MS for both catalysts coated on the concrete blocks are: ethyl benzene (C_8H_{10}), benzaldehyde (C_6H_5CHO) and hexadecane ($C_{16}H_{34}$). Some of these products are oxidized to carbon dioxide and water through degradation reactions. This result was different from that found by Wang & Ray [38] and Hinjosa-Reyes *et al.* [39] except benzaldehyde it has reported as well as one detected in this study. In their study, benzyl alcohol, benzaldehyde and benzoic

TABLE-3
PRODUCTS OF TOLUENE PHOTODEGRADATION WITH A CONFIDENT OF MORE THAN 98 % USING THE NIST LIBRARY AS IDENTIFIED FROM GC-MS ANALYSIS

Peak number	Compound Name	Retention time (min)	Molecular formula	Toxicological information
1	Ethylbenzene	7.690	C_8H_{10}	Safety
2	Benzaldehyde	9.281	C_6H_5CHO	Safety
3	Hexadecane	13.750	$C_{16}H_{34}$	Safety

acid were formed on the surface of catalyst during photocatalytic degradation of toluene. From these results can be observed, that the CH_3 group enhanced the reactivity of toluene molecule and it may be easily oxidized through the photocatalytic process. However, the aromatic ring was still hard to be destroyed to generate different compounds. Alberici and Jardim [40] also obtained similar results and made the degradation of toluene possible through photocatalytic reduction by introducing methanol as electron donor. Dong *et al.* [41] reported that the degradation of toluene could achieve in a high air humidity (more than 50 %) through photocatalytic reduction, H_2O acted as an electron donor to capture the photogenerated hole. The products resulting from the decomposition of toluene previously are non-carcinogenic and safer than toluene according to Material Safety Data Sheet (MSDS) system.

The suggested mechanism of the photocatalytic degradation of toluene on the TiO_2 and $LiNbO_3$ follows three steps: (1) the adsorption of toluene molecules onto the surface of the catalysts; (2) a fast degradation by the light irradiation of UV, which includes the production of electron-hole pairs, free radicals and then oxidation; the photogenerated conducted band electrons were trapped by oxygen molecules, leading to the formation of radicals such as $O_2^{\bullet}$, $HCOO^{\bullet}$ and $^{\bullet}OH$ to produce active oxidizing species, usually free radicals ($^{\bullet}OH$) in presence of air, but also dissociated neutral oxygen species ($O^{\bullet}$) [42]. These free radicals with a high oxidation potential were the predominant species contributing to the degradation of the toluene; (3) the TiO_2 and $LiNbO_3$ photocatalytic free radical oxidation of toluene can also proceed in a different way, giving rise to the gas-phase intermediate organic products with TiO_2 and $LiNbO_3$ under complex light irradiation of UV-light [43].

Influence of toluene adsorption and degradation on micro-structures of photocatalyst: The prepared samples were magnified using scanning electron microscope (SEM) to reveal the different in the microscopic features on the surface obtained before and after of the toluene adsorption. In this process, different locations in the sample were captured at a low magnification rate and were then repetitively enlarged at higher magnification rates. The structure of the particles of TiO_2 and $LiNbO_3$ that's coated on the surface of concrete blocks were observed. Most of the scanning was made with 20KX magnification and 10 kV scanning voltage.

Fig. 8 illustrated the SEM photomicrograph of the TiO_2 before and after toluene adsorption on the concrete surfaces. A dense structure with a uniformly distributed layer was observed in TiO_2. The morphology of the particles is a spherical, brighter and systematic. The result also showed that the morphology of sample surfaces and TiO_2 particles after adsorbed toluene; the surfaces of the samples were very coarse. At larger magnification, it is obvious that the TiO_2 particles were almost having a large reaction surface. The particles are larger agglomerates in which appeared clearly in the forms of the particle structures of TiO_2. From the SEM images of $LiNbO_3$ (Fig. 9), individual particles in the cubical and systematical shape before adsorption can be observed. In contrast to $LiNbO_3$ that was characterized with a clear surface, coated $LiNbO_3$ in Fig. 9 was seen with adsorption of toluene on the concrete block surfaces. Similarly, a comparison with the SEM image of TiO_2 it is also appeared that $LiNbO_3$ particles agglomerating on external surface of concrete block which is similar to the result reported by Nath and Zain [44] in their study of using $LiNbO_3$ as doped and coated catalyst, other studied was conducted on photodegradation polyphenols by Nath *et al.* [28] using photocatalyst and Sn^{3+}, Fe^{3+} doped, the SEM images of adsorbents appeared high agglomerate surface. The observer of the roughness can be attributed to the amount of photocatalyst which is covered by a thick dense of catalyst layer.

Conclusion

TiO_2 and $LiNbO_3$ are very effective for the decomposition of toluene, which is an indoor pollutant. Based on this study, a test was carried out in which appropriate amount of toluene was injected in a fixed bed reactor under UV-irradiation. The samples were analyzed by chromatography analysis apparatus for measuring the performance of photocatalytic concrete products to removal of toluene. Experimental conditions that affect the photocatalytic oxidation were identified in this study. The Langmuir-Hinshelwood model has been studied and applied to photocatalytic oxidation comprehensively. It was also successfully applied to describe the adsorption and photodegradation

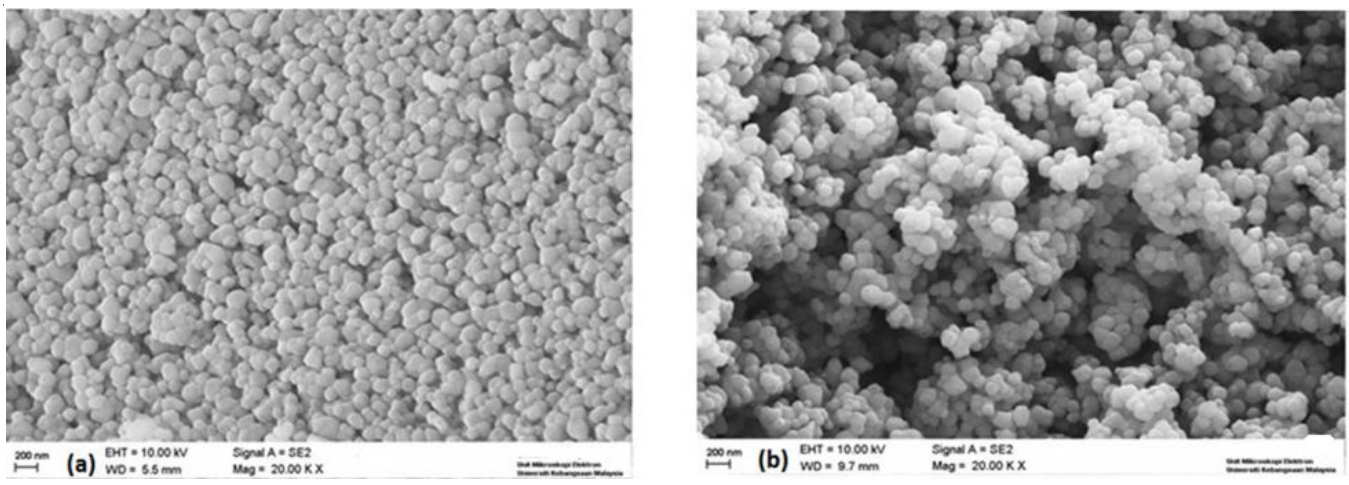

Fig. 8. SEM photomicrograph of the titanium dioxide $LiNbO_3$ thin layer: (a) before adsorption and (b) after adsorption target pollutants on the concrete block surfaces. Magnification: 20 kA; Scale bar: 200 nm

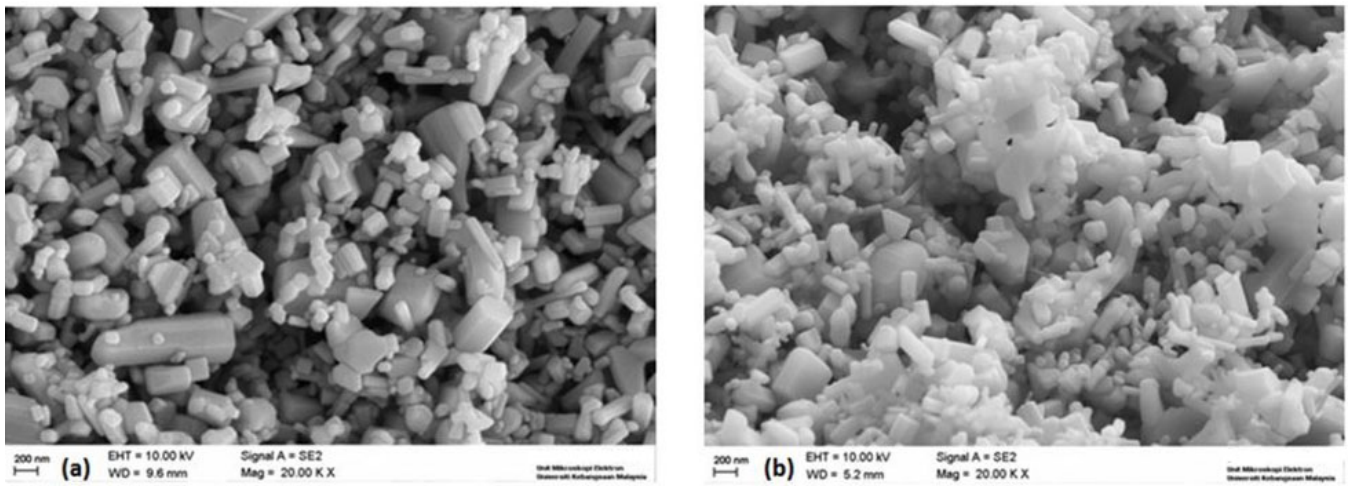

Fig. 9. SEM photomicrograph of the zinc oxide and TiO_2 thin layer: (a) before adsorption and (b) after adsorption target pollutants on the concrete block surfaces. Magnification: 20 KX; Scale bar: 200 nm

reaction rate of toluene. The experimental results indicate that the $LiNbO_3$ has advanced effect on the photocatalytic oxidation of toluene than TiO_2. Additionally, it was observed that toluene can be easily degraded through photocatalysis in the presence of UV-light, and the reaction rate of $LiNbO_3$ samples was much faster than that of TiO_2 under the same conditions. Lower initial concentration of toluene shows advanced toluene decomposition than high concentration. However, a longer reaction time is needed for the photocatalytic oxidation of toluene with high and low concentrations. SEM photomicrograph of TiO_2 and $LiNbO_3$ illustrated enhanced photocatalytic activities of both catalysts for pollutant removal. The result appeared a much rougher surface was observed after adsorption for all samples. Furthermore, the influence of TiO_2 and $LiNbO_3$ surface layer porosity on toluene adsorption was affected by the type of materials with which they were prepared. The results also show that the toluene removal decreased with age, but the decrease stabilized at the age of 5-7 h. $LiNbO_3$ was showing better photocatalytic performance than TiO_2; hence, it is one of the best photocatalytic ability for improving indoor air quality.

ACKNOWLEDGEMENTS

The authors acknowledge the Fundamental Research Grant Scheme FRGS/1/2016/TK06/UKM/01/1 of Universiti Kebangsaan Malaysia and the Ministry of Education, Malaysia.

REFERENCES

1. B. Marco and D. Schaffer, *Concr. Int.*, **31**, 49 (2009).
2. O. Geiss, C. Cacho, J. Barrero-Moreno and D. Kotzias, *Build. Environ.*, **48**, 107 (2012); https://doi.org/10.1016/j.buildenv.2011.08.021.
3. C.Y.H. Chao, *Build. Environ.*, **36**, 999 (2001); https://doi.org/10.1016/S0360-1323(00)00057-3.
4. R.K. Nath, M.F.M. Zain and M. Jamil, *Renew. Sustain. Energy Rev.*, **62**, 1184 (2016); https://doi.org/10.1016/j.rser.2016.05.018.
5. A.P. Jones, *Soc. Sci. Med.*, **47**, 755 (1998); https://doi.org/10.1016/S0277-9536(98)00151-8.
6. K. Kovler and N. Roussel, *Cement Concr. Res.*, **41**, 775 (2011); https://doi.org/10.1016/j.cemconres.2011.03.009.
7. R.L. Laumbach, Sick Building Syndrome, In: International Encyclopedia of Public Health, pp. 4-8 (2008).
8. J.M. Seltzer, Occupational Medicine: Effects of the Indoor Environment on Health, Hanley & Belfus: Philadelphia, vol. 10, p. 26 (1995).
9. H.I. Zeliger, Sick Building Syndrome, In: Human Toxicology of Chemical Mixture, edn 2, pp. 143-158 (2011).
10. S. Tomaziè, V. Logar, Z. Kristl, A. Krainer, I. Skrjanc and M. Kosir, *Build. Environ.*, **70**, 60 (2013); https://doi.org/10.1016/j.buildenv.2013.08.026.
11. A. Mills and S. Le Hunte, *J. Photochem. Photobiol. Chem.*, **108**, 1 (1997); https://doi.org/10.1016/S1010-6030(97)00118-4.
12. T. Noguchi, A. Fujishima, P. Sawunyama and K. Hashimoto, *Environ. Sci. Technol.*, **32**, 3831 (1998); https://doi.org/10.1021/es980299+.
13. E. Obuchi, T. Sakamoto, K. Nakano and F. Shiraishi, *Chem. Eng. Sci.*, **54**, 1525 (1999); https://doi.org/10.1016/S0009-2509(99)00067-6.
14. J.C. Yu, J. Yu, W. Ho and J. Zhao, *J. Photochem. Photobiol. Chem.*, **148**, 331 (2002); https://doi.org/10.1016/S1010-6030(02)00060-6.
15. R.K. Nath, M.F.M. Zain and A.A.H. Kadhum, *The Scientific World J.*, Article ID 686497 (2013); https://doi.org/10.1155/2013/686497.
16. Y. Zhang, R. Yang and R. Zhao, *Atmos. Environ. Int.*, **37**, 3395 (2003); https://doi.org/10.1016/S1352-2310(03)00357-1.
17. E. Palomares, A. Uzcátegui, C. Franch and A. Corma, *Appl. Catal. B*, **142–143**, 795 (2013); https://doi.org/10.1016/j.apcatb.2013.06.015.
18. J. Chen and C. Poon, *Environ. Sci. Technol.*, **43**, 8948 (2009); https://doi.org/10.1021/es902359s.
19. C. Akly, P.A. Chadik and D.W. Mazyck, *Appl. Catal. B*, **99**, 329 (2010); https://doi.org/10.1016/j.apcatb.2010.07.002.
20. K. Demeestere, J. Dewulf, B. De Witte, A. Beeldens and H. Van Langenhove, *Build. Environ.*, **43**, 406 (2008); https://doi.org/10.1016/j.buildenv.2007.01.016.
21. D. Farhanian and F. Haghighat, *Build. Environ.*, **72**, 34 (2014); https://doi.org/10.1016/j.buildenv.2013.10.014.
22. A. Fujishima and X.T. Zhang, *C.R. Chim.*, **9**, 750 (2006); https://doi.org/10.1016/j.crci.2005.02.055.
23. R.K. Nath, M.F.M. Zain and A.A.H. Kadhum, *Adv. Nat. Appl. Sci.*, **6**, 1030 (2012).
24. G.L. Guerrini, *Constr. Build. Mater.*, **27**, 165 (2012); https://doi.org/10.1016/j.conbuildmat.2011.07.065.
25. M. Safari, M. Rostami, M. Alizadeh, A. Alizadehbirjandi, S.A. Nakhli and R. Aminzadeh, *Iran. J. Environ. Health Sci. Eng.*, **12**, 1 (2014); https://doi.org/10.1186/2052-336X-12-1.
26. W.W. Nazaroff, *Indoor Air*, **23**, 353 (2013); https://doi.org/10.1111/ina.12062.
27. M. Stock and S. Dunn, *IEEE Trans. Ultrason. Ferroelectr. Freq. Control*, **58**, 1988 (2011); https://doi.org/10.1109/TUFFC.2011.2042.

28. R.K. Nath, M.F.M. Zain, A.A.H. Kadhum and A.B.M.A. Kaish, *Constr. Build. Mater.*, **54**, 348 (2014); https://doi.org/10.1016/j.conbuildmat.2013.12.072.
29. S.B. Kim and S.C. Hong, *Appl. Catal. B*, **35**, 305 (2002); https://doi.org/10.1016/S0926-3373(01)00274-0.
30. Y. Ku, C. Ma and Y.S. Shen, *Appl. Catal. B*, **34**, 181 (2001); https://doi.org/10.1016/S0926-3373(01)00216-8.
31. J. Zhao and X. Yang, *Build. Environ.*, **38**, 645 (2003); https://doi.org/10.1016/S0360-1323(02)00212-3.
32. Y. Zhang, R. Yang, Q. Xu and J. Mo, *J. Air Waste Manage. Assoc.*, **57**, 94 (2007); https://doi.org/10.1080/10473289.2007.10465302.
33. P. Pichat, J. Disdier, C. Hoang-Van, D. Mas, G. Goutailler and C. Gaysse, *Catal. Today*, **63**, 363 (2000); https://doi.org/10.1016/S0920-5861(00)00480-6.
34. A. Di Paola, E. García-López, S. Ikeda, G. Marcì, B. Ohtani and L. Palmisano, *Catal. Today*, **75**, 87 (2002); https://doi.org/10.1016/S0920-5861(02)00048-2.
35. C. Yu, Deactivation and Regeneration of Environmentally Exposed Titanium Dioxide (TO_2) based Products, Edited by E183413 DORN. Hong Kong: Testing Report for Environmental Protection Department, HKSAR (2003).
36. C.S. Chuang, M.K. Wang, C.H. Ko, C.C. Ou and C.H. Wu, *Bioresour. Technol.*, **99**, 954 (2008); https://doi.org/10.1016/j.biortech.2007.03.003.
37. T. Sano, N. Negishi, K. Takeuchi and S. Matsuzawa, *Sol. Energy*, **77**, 543 (2004); https://doi.org/10.1016/j.solener.2004.03.018.
38. J.H. Wang and M.B. Ray, *Sep. Purif. Technol.*, **19**, 11 (2000); https://doi.org/10.1016/S1383-5866(99)00078-7.
39. M. Hinojosa-Reyes, V. Rodríguez-González and S. Arriaga, *J. Hazard. Mater.*, **209-210**, 365 (2012); https://doi.org/10.1016/j.jhazmat.2012.01.035.
40. R.M. Alberici and W.F. Jardim, *Appl. Catal. B*, **14**, 55 (1997); https://doi.org/10.1016/S0926-3373(97)00012-X.
41. H.K. Dong, H.C. Dong, S.Y. Myoung and W.K. Kwang, *J. Adhes. Sci. Technol.*, **27**, 683 (2013); https://doi.org/10.1080/01694243.2012.690661.
42. A. Bouzaza and A. Laplanche, *J. Photochem. Photobiol. Chem.*, **150**, 207 (2002); https://doi.org/10.1016/S1010-6030(02)00088-6.
43. N. Sobana and M. Swaminathan, *Sol. Energy Mater. Sol. Cells*, **91**, 727 (2007); https://doi.org/10.1016/j.solmat.2006.12.013.
44. R.K. Nath and M.F.M. Zain, *Adv. Environ. Biol.*, **9**, 1 (2015).